Title	Detection of ultra-low protein concentrations with the simplest possible field effect transistor
Authors	Georgiev, Yordan M.;Petkov, Nikolay;Yu, Ran;Nightingale, Adrian M.;Buitrago, Elizabeth;Lotty, Olan;DeMello, John C.;Ionesco, Adrian M.;Holmes, Justin D.
Publication date	2019-05-08
Original Citation	Georgiev, Y. M., Petkov, N., Yu, R., Nightingale, A. M., Buitrago, E., Lotty, O., deMello, J. C., Ionescu, A. and Holmes, J. D. (2019) 'Detection of ultra-low protein concentrations with the simplest possible field effect transistor', Nanotechnology, 30 (32), 324001 (8 pp). doi: 10.1088/1361-6528/ab192c
Type of publication	Article (peer-reviewed)
Link to publisher's version	https://iopscience.iop.org/article/10.1088/1361-6528/ab192c/meta - 10.1088/1361-6528/ab192c
Rights	© 2019 IOP Publishing Ltd. This is an author-created, un-copyedited version of an article accepted for publication in Nanotechnology The publisher is not responsible for any errors or omissions in this version of the manuscript or any version derived from it. The Version of Record is available online at https://doi.org/10.1088/1361-6528/ab192c . - https://creativecommons.org/licenses/by-nc-nd/3.0/
Download date	2023-04-02 00:04:07
Item downloaded from	http://hdl.handle.net/10468/7934

Detection of ultra-low protein concentrations with the simplest possible field effect transistor

Yordan M. Georgiev[1,2,*,‡], Nikolay Petkov[1,2], Ran Yu[1], Adrian M. Nightingale[3], Elizabeth Buitrago[4], Olan Lotty[1,2], John C. deMello[3], Adrian Ionescu[4], and Justin D. Holmes[1,2]

[1] Materials Chemistry & Analysis Group, Department of Chemistry and Tyndall National Institute, University College Cork, Lee Maltings, Dyke Parade, Cork, Ireland; One
[2] Centre for Research on Adaptive Nanostructures and Nanodevices (CRANN/AMBER), Trinity College Dublin, Dublin 2, Ireland
[3] Imperial College London, South Kensington, London SW7 2AZ, United Kingdom
[4] Nanoelectronic Devices Laboratory (Nanolab), École Polytechnique Fédéral de Lausanne (EPFL), Station 11, Bâtiment ELB 336, CH-1015 Lausanne, Switzerland
[*] Corresponding author; present address: Institute of Ion Beam Physics and Material Research, Helmholtz-Zentrum Dresden-Rossendorf, Bautzner Landstraße 400, 01328 Dresden, Germany
[‡] On leave of absence from the Institute of Electronics at the Bulgarian Academy of Sciences, 1784 Sofia, Bulgaria.

E-mail: **y.georgiev@hzdr.de**

Received xxxxxx
Accepted for publication xxxxxx
Published xxxxxx

Abstract

Silicon nanowire (Si NW) sensors have attracted great attention due to their ability to provide fast, low-cost, label-free, real-time detection of chemical and biological species. Usually configured as field effect transistors (FETs), they have already demonstrated remarkable sensitivity with high selectivity (through appropriate functionalisation) towards a large number of analytes in both liquid and gas phases. Despite these excellent results, Si NW FET sensors have not yet been successfully employed to detect single molecules of either a chemical or biological target species. Here we show that sensors based on silicon junctionless nanowire transistors (JNTs), the simplest possible transistors, are capable of detecting the protein streptavidin at a concentration as low as 580 zM closely approaching the single molecule level. This ultrahigh detection sensitivity is due to the intrinsic advantages of junctionless devices over conventional FETs. Apart from their superior functionality, JNTs are much easier to fabricate by standard microelectronic processes than transistors containing *p*-*n* junctions. The ability of JNT sensors to detect ultra-low concentrations (in the zeptomolar range) of target species, and their potential for low-cost mass production, will permit their deployment in numerous environments, including life sciences, biotechnology, medicine, pharmacology, product safety, environmental monitoring and security.

Keywords: Si nanowire biosensor, junctionless nanowire transistor, ultrahigh detection sensitivity, protein, streptavidin, single-molecule detection

1. Introduction

Since their inception in 2001 [1], silicon nanowire (Si NW)-based field effect transistors (FETs) have been extensively studied as chemical and biosensors due to their superb electrical and mechanical properties and their large surface-to-volume ratios. The sensing mechanism has largely been based on the interaction of electrically charged particles (molecules) of the target analyte with a nanowire surface (see figure 1(a)). These charged molecules effectively play the role of a top gate, changing the electrical conductance of the nanowire (transistor channel). In such a way, the interactions of molecules with the nanowires are directly converted into easily detectable electrical signals. Because of the very small cross-section of the nanowires (and the large surface area to volume ratio), even a few charged molecules attached to the nanowire surface are able to effectively modulate the FET current (channel conductance) and generate a sensor signal. Indeed, Si NW-based sensors have already demonstrated excellent sensitivity in both liquid [2] and gas [3] phases. Using FETs built from grown Si NWs, Patolsky et al. [4] have shown detection of single influenza type A viruses. Stern et al. [5] managed to detect the protein streptavidin at concentrations as low as 10 fM using top-down fabricated Si NW sensors. In our recent paper [6] we have reported on sensing the same protein at even lower concentration, 17 aM, implementing 3D vertically stacked Si NW FETs. To the best of our knowledge, this is the lowest protein concentration detected to date. Although these results are really impressive, there is yet no report on the detection of any species at the single molecule level using Si NW FET-based sensors. The most probable reason limiting the detection sensitivity of these sensors is the inherent low-frequency noise of semiconductor FETs, which is caused by resistance fluctuations and is known as flicker noise or 1/f noise. The ratio of the sensor signal to this noise (signal to noise ratio, SNR) is suggested to determine the detection limit of the sensors [7].

Recent studies [8, 9] have shown that in the case of Si NW-FET sensors the 1/f noise does not originate in the nanowire itself but is mainly generated in the oxide on top of the Si NW (the gate oxide) via trapping and releasing of charge carriers at trap states near the semiconductor-oxide interface. Pud et al. [9] demonstrated that the noise can be reduced by moving the conducting channel away from the top dielectric layer to the bulk of the Si NW, with the help of an appropriate back-gate potential. They used this effect for tuning the FET operation mode to increase the sensitivity of the fabricated biosensor structure by 50% and suggested that their results reflected a novel way to improve the sensitivity of biosensors by designing devices with controlled channel positioning.

Due to their specific architecture and conduction mechanism, junctionless nanowire transistors (JNTs) [10] naturally meet the above mentioned requirements for ultimate sensor sensitivity: even in the subthreshold mode, their conduction channel is positioned not at the surface close to the semiconductor-oxide interface as in the standard FETs but near the centre of the nanowire. JNTs have been proposed as a disruptive alternative of conventional metal-oxide-semiconductor field-effect transistors (MOSFETs) [10]. A JNT is essentially a gated resistor where the source, channel and drain have the same type of doping without any dopant concentration gradient (figure 1(a)). In the absence of the p-n junctions commonly found in MOSFETs, the current flow in a JNT is entirely determined by the gate potential, which controls the carrier density in the channel. Therefore, there are two important characteristic features of properly functioning JNTs: (i) the cross-section of the transistor channel is small enough to achieve full depletion of charge carriers in the off-state and (ii) heavy doping (up to $1\text{-}5\times10^{19}$ cm^{-3}) of the whole device (source, channel and drain) for high on-state currents. The JNT is the simplest transistor structure possible and probably the most scalable of all FET structures. Such a device is easier to fabricate than standard MOSFETs, since it does not require separate doping of source and drain regions and the very challenging formation of abrupt ultra-shallow p-n junctions. This fact, together with the number of performance advantages over MOSFETs [10, 11, 12, 13], has quickly attracted a vast interest in JNTs. However, their application as sensors, although very appealing, has not yet been extensively studied.

Currently, there are two main concepts for achieving the ultimate sensitivity (detection limit) with Si NW FET-type sensors: operating them (i) in the subthreshold mode [14] or (ii) in the above-threshold mode [7]. The operation mode of the sensors can be set by applying an appropriate back-gate potential, at the expense of increased power consumption. In the case of JNTs, however, their performance depends strongly on the geometry (height, width, and length) of the channel (NW) as well as on its doping level. Therefore, these parameters can be used to finely tune the operation point of devices into the appropriate mode without having to use an additional power supply, which makes them very energy efficient [15].

We have already implemented JNT-based devices as chemical and biological sensors. A series of experiments for sensing the ionic strength and the pH value of buffer solutions have proven the excellent sensitivity of these sensors [13, 16, 17]. In the present work we demonstrate sensing of the protein streptavidin at a concentration as low as 580 zM, which is by far the lowest concentration of this protein that has been detected to date and corresponds to detection in the range of only few molecules.

2. Experimental

The sensors were fabricated on silicon-on-insulator (SOI) wafers. Device layout and images of sample devices are shown in figure 1(b). To render the fabricated sensors sensitive exclusively to the protein streptavidin, the Si nanowires were functionalised with biotin. Their electrical characterisation was performed using a cascade manual probe station, both under dry and liquid conditions. Fluid delivery to devices was arranged with polydimethylsiloxane (PDMS) stamps (figure 2), polytetra-fluoroethylene (PTFE) tubing and a syringe pump. Details are given in the subsections below.

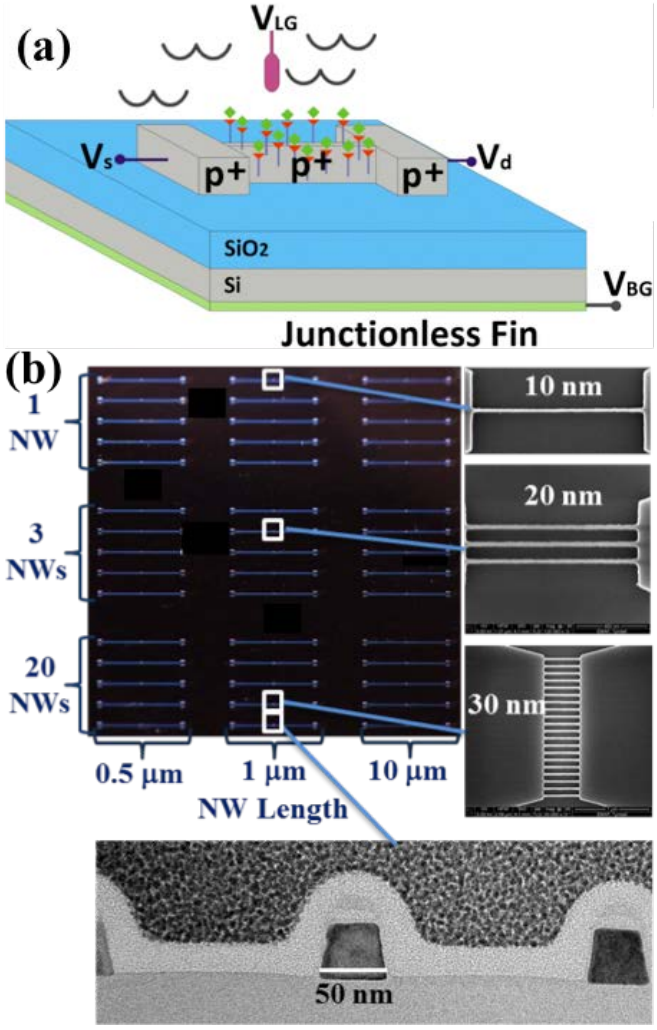

Figure 1. Junctionless nanowire transistors (JNTs) as chemo-/biosensors. (a) Schematic presentation of a JNT sensor fabricated on a SOI wafer. (b) Optical microscopy image of an SOI chip with nine groups of different JNT sensor together with an SEM top views and a TEM cross-sectional view of individual devices having 1, 3, or 20 nanowires of different lengths (0.5 and 1 µm) and widths (10, 20, 30, and 50 nm).

2.1 Fabrication of Junctionless Si NW Devices

JNT sensors with various nanowire widths (10, 20, 30, and 50 nm), lengths (0.5, 1, and 10 µm) and numbers (1, 3, and 20 NWs) were fabricated on highly p-doped (10^{18} cm^{-3}) SOI wafers with top Si device layer of 45 nm and buried oxide (BOX) layer of 145 nm SiO_2 (see figure 1(b)). The patterning was done with electron beam lithography (EBL) using a high-contrast and low roughness development process for the negative tone resist hydrogen silsesquioxane (HSQ) [18, 19], followed by a chlorine (Cl_2) chemistry based reactive ion etching (RIE). Then an additional 200 nm SiO_2 layer was deposited on the whole surface except the device regions, to minimise the leakage current through the BOX. Next, the source/drain metal contacts, interconnects and contact pads were created by deposition of a 100 nm thick nickel (Ni) layer and thermal annealing for 30 min at 400 °C in forming gas (10% H_2 / 90 % N_2). These two subsequent depositions were done by electron beam evaporation and were respectively combined with two steps of photolithography and lift-off. A final third step of photolithography was performed with 2 µm thick negative photoresist SU8, which was used to passivate the whole surface of the chips, except the device regions and the metal contact pads. The fabricated devices were inspected by both optical and scanning electron microscopes (SEM). Detailed description of the fabrication process is given elsewhere [17].

2.2 NW surface modification

To make the JNT sensors sensitive only to the protein streptavidin, the Si nanowires were functionalised with biotin. Streptavidin has a high affinity for biotin and they form a very strong non-covalent binding. The functionalisation was done in several steps. First, the SiOx nanowire surface was treated in a piranha solution (3:1 H_2SO_4:H_2O_2) to produce a clean hydroxyl-terminated surface. Next (3-Aminopropyl)triethoxysilane (APTES) was covalently attached to the nanowire surface by immersing the samples in a solution of 5 v/v % APTES in anhydrous toluene for 3 hours at 50 °C. Then the samples were rinsed with anhydrous toluene, deionised (DI) water and dried under nitrogen (N_2). The aminosilanised nanowires (Si-APTES) were subsequently immersed for three hours at room temperature in 2 mL phosphate buffered saline (PBS, pH 7.4) with added 100 µL of E,Z link-NHS-LC-Biotin in dimethylformamide (DMF) (1 mg/mL). During this time, the NHS-LC-Biotin reacts with the primary amine of the surface-tethered silane to leave a biotinylated surface. Finally, surfaces were rinsed with PBS and DI water and dried under nitrogen. Contact angle measurements changed from 19° (highly hydrophilic) to ~70° (less hydrophilic), indicating successful surface modification.

2.3 Electrical characterisation and fluid delivery

The electrical characterisation was done at room temperature using a cascade manual probe station, and an Agilent B1500 semiconductor parameter analyser.

Efficient fluid delivery to the sensors was enabled by bonding polydimethylsiloxane (PDMS) stamps with a 150 µm-width channel to the front surface of the chips (figures 2(a), 2(b)). Inlet/outlets access holes with diameters ~ 400 µm were drilled on the top of the stamp to link the microfluidic channel to external PTFE tubing (figures 2(a), 2(b)). The tubing was relatively long (~ 1.5 m) to enable administration and collection of the fluid from the outside of the probe station. The solutions containing the target analyte were delivered to each sensor at a rate of 100 µL/min with a syringe (BD Plastipak, 10 mL) propelled by a pump (Harvard, Pump 11+). From the syringe, the flow passed through PTFE tubing with inner diameter (ID) of 0.4 mm and outer diameter (OD) of 1.0 mm. Approximately 10 cm from exiting the syringe, the flow passed through a T-junction where a small amount of a different solution could be added into the main fluid flow as required. From the T-junction the flow continued along the PTFE tubing (~1 m) into the probe station. Standard fittings from Upchurch Scientific were used for all connections. Inside the probe station the tubing was downsized to OD 0.4 mm and ID 0.1 mm PTFE tubing using interconnect junctions fabricated in-house from PDMS. The smaller tubing was required to interface to the PDMS stamp but could not be used for the entire length of the fluid supply lines, as excessive backpressure would be generated. The Si NWs were accessible through the small windows on the SU-8 passivation layer.

In some of the measurements under 'liquid conditions', an Ag/AgCl reference electrode (ALS RE-1S, 4 mm barrel diameter) was used to maintain a constant liquid potential. The reference electrode was incorporated into a flow cell and attached to the microfluidic channels by the PTFE tubing. The flow cell consists of a small volume chamber (~1 µL) at the base of the electrode, which is supplied via a 1 mm diameter channel custom made in PDMS (figure 2(c)).

3. Results and discussion

Figure 1(b) shows an optical microscope image of a single SOI chip containing 45 different nanowire devices as well as a top SEM view of devices having 10, 20 and 30 nm NW width together with a transmission electron microscope (TEM) cross-sectional view of a device with 50 nm NWs. The images clearly demonstrate the excellent results of the patterning process, which delivered very smooth nanowires with dimensions closely matching the designed ones. This is an important prerequisite for the good performance of the sensing devices.

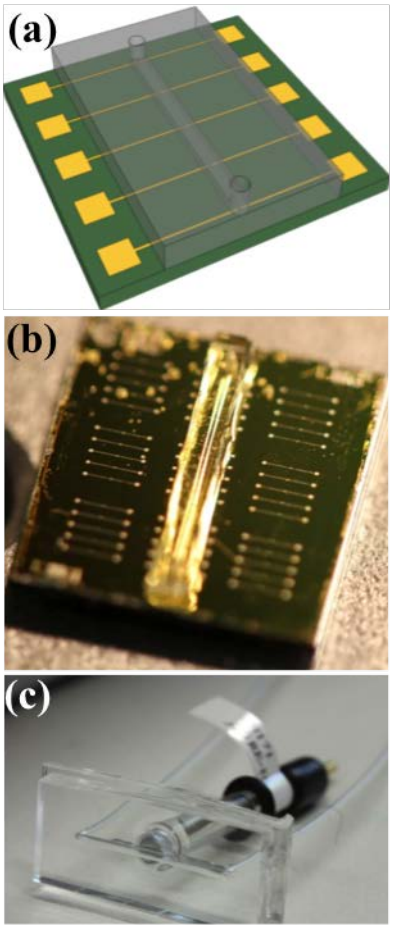

Figure 2. *Microfluidic cannels. (a) Schematic presentation of a group of 5 JNT sensors with a PDMS stamp containing a microfluidic channel. (b) Optical microscopy image of an SOI chip with nine groups of different JNT sensor and a PDMS stamp with a microfluidic channel bonded on top of three of the device groups. (c) Ag/AgCl reference electrode incorporated into a flow cell.*

3.1 Electrical characterisation of the fabricated devices

To check the quality of the fabricated and biotinylated sensors, they were first electrically tested under dry conditions. Figure 3(a) shows a sample transfer characteristics of a device constructed from a single nanowire with a diameter of 50 nm and length of 1 µm. The drain current I_d was measured as a function of the back-gate potential V_{bg} by sweeping V_{bg} forward (circles) and backward (triangles) between -20 V and 10 V while keeping the drain potential V_d constant at V_d = 1 V. The two transfer characteristics overlap well, indicating the high quality of the fabricated sensors. The threshold voltage V_{th} shifts slightly towards the right indicating a small negative charge accumulation. Injected interface charges, which do not dissipate as the gate bias polarity changes, lead to a shift in the threshold voltage [20]. Hysteresis can affect the stability

of the sensors causing short- and long-term drift of the sensor response [21]. The little hysteresis observed here (< 0.33 V of the back-gate potential) indicates small defect-induced charge trapping at the interface Si/SiO_2 [22].

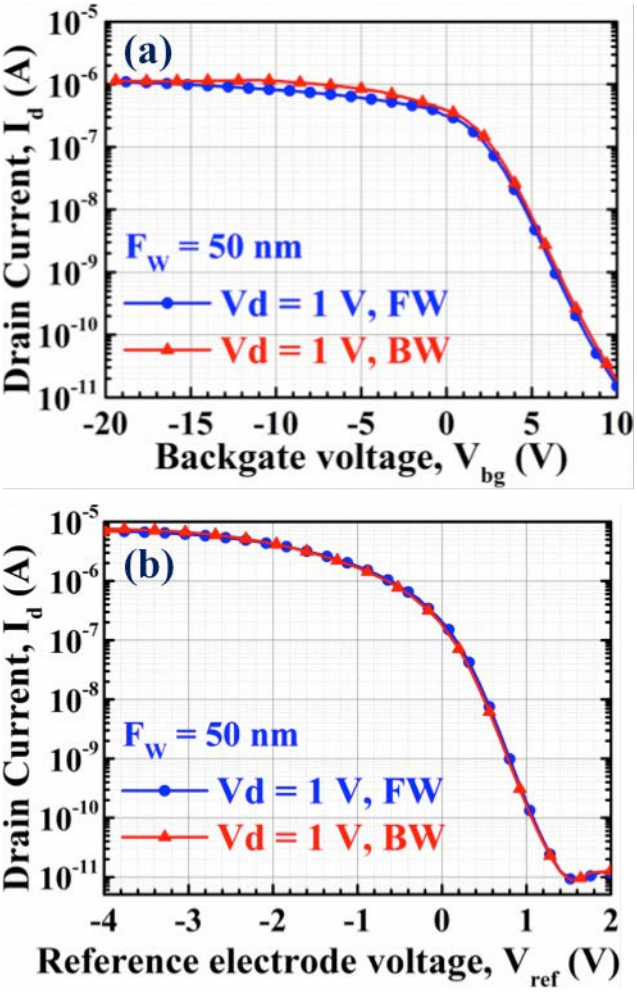

Figure 3. Results of electrical measurements of the sensors. (a) Transfer characteristics (I_d-V_{bg} curves under dry conditions) of a device having a single 50 nm nanowire of 1 µm length. The drain current I_d was measured while sweeping the back-gate potential V_{bg} forward (circles) and backward (triangles) between -20 and 10 V at constant drain potential V_d = 1 V. (b) Transfer characteristics (I_d-V_{ref} curves under constant PBS flow) of a device having an array of 20 nanowires of 50 nm width and 10 µm length. The drain current I_d was measured while sweeping the reference electrode potential V_{ref} forward (circles) and backward (triangles) between -4 and 2 V at a constant drain potential of V_d = 1 V.

As a next step, a similar measurement was done while continuously flowing (100 µL/min) PBS through the microfluidic channels aligned over the sensors. The PBS potential was controlled by the reference electrode. Figure 3(b) presents sample transfer characteristics of a device having an array of 20 nanowires of 50 nm width and 10 µm length. The drain current I_d was measured as a function of the reference electrode potential V_{ref} by sweeping V_{ref} forward (circles) and backward (triangles) between -4 V and 2 V while maintaining a constant drain potential of V_d = 1 V. Here the two transfer characteristics overlap almost perfectly, which is yet another demonstration of the excellent quality of the fabricated and functionalised sensors.

3.2 Sensing experiments

In this work, streptavidin-biotin has been chosen as a model target-probe pair, with streptavidin in solution being sensed using biotin covalently tethered to the NW surface. This target-probe pair is well known, has one of the strongest non-covalent binding interactions in nature, and very fast association kinetics. It is widely used for evaluation of the sensing performance of various sensors and is, therefore, appropriate for comparison of different sensor concepts. The Si nanowires functionalisation with biotin is described in section 2.2.

In the first series of streptavidin sensing experiments, the drain current I_d was measured as a function of the back-gate potential V_{bg} by sweeping V_{bg} forward and backward between -20 and 5 V ten times at constant drain potential V_d = 1 V while continuously flowing (100 µL/min) plain PBS over biotinylated sensors. The measurements of a device with an array of 20 NWs of 0.5 µm length and 50 nm width resulted in on-currents I_{on} of ~ 1.5 µA and off-currents I_{off} of ~ 0.15 nA (I_{on}/I_{off} ratio of ~ 10^4) as shown in figure 6(a). Then PBS solution with relatively high concentration of streptavidin (0.4 µM) was flowed at the same rate over the sensors instead of the pure PBS and again a series of ten consequent I_d-V_{bg} measurements was done at identical conditions. The obtained I_d-V_{bg} curves for the same device have an obviously much smoother subthreshold slope (SS) and much higher currents, I_{on} ~ 10 µA and I_{off} ~ 0.1 µA (I_{on}/I_{off} ratio of ~ 10^2), see figure 6(a). These results indicate successful binding of streptavidin molecules to the biotinylated NW surfaces. Since streptavidin has a weakly acidic isoelectric point (pI ~ 5.6) [22], its molecules are negatively charged when dissolved in a PBS solution of pH = 7.4, as in our case. Their binding to the nanowire surfaces acts as a negative gating of the sensor and caused accumulation of majority carriers (holes) in the p-type device channel. Therefore, a significant increase of drain current was observed: up to a factor of 10 for the I_{on} and a factor of 10^3 for the I_{off} (figure 4(a)).

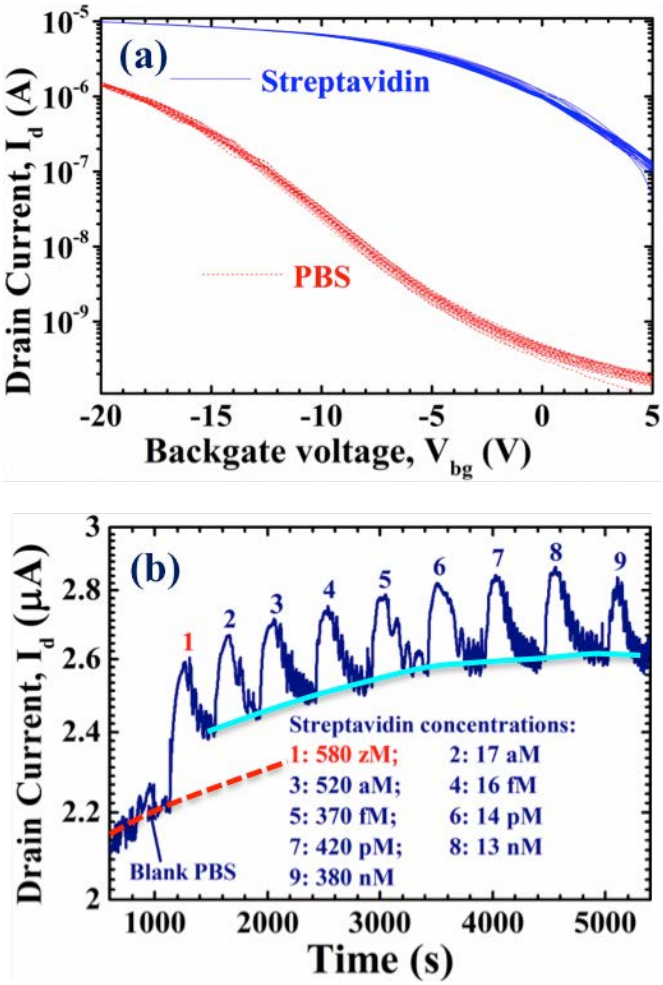

Figure 4. Results of the sensing experiments. (a) Transfer characteristics (I_d-V_{bg} curves under constant flow of pure PBS or PBS with high concentration of streptavidin) of a biotinylated device having an array of 20 NWs of 0.5 μm length and 50 nm width. The drain current I_d was measured while sweeping the back-gate potential V_{bg} forward and backward ten times between -20 and 5 V at constant drain potential V_d = 1 V. (b) Time dependence of drain current I_d for a biotinylated sensor having an array of 20 nanowires of 50 nm width and 10 μm length and biased at V_{ref} = -1.5 V and V_d = 1 V. The drain current I_d was measured under a steady stream of pure PBS (100 μl/min) with periodical injections of small amounts (100 μL) of PBS solutions with increasing streptavidin concentrations (shown in the figure). The dashed line (red online) extrapolates the possible current drift before the first streptavidin injection, while the solid line (light blue online) connects the "valley" current values after each streptavidin injection.

As a final step, solutions of different streptavidin concentrations in PBS (pH = 7.4) were prepared from a solution with an initial molarity of ~380 nM by consecutively diluting it in PBS by a factor of 30 eight times until an extremely low molarity of ~580 zM (580×10^{-21} M) was achieved. During the sensing experiment, a steady stream of pure PBS was flowed through the microfluidic channel at a rate of 100 μL/min and periodically small amounts (100 μL) of nine different solutions with increasing streptavidin concentrations (580 zM, 17 aM, 520 aM, 16 fM, 370 fM, 14 pM, 420 pM, 13 nM and 380 nM) were administered one by one into this steady stream, while continuously measuring the drain current I_d of the sensing device. The reference electrode was used to maintain constant potential of the solutions. In figure 4(b), I_d of a biotinylated sensors having an array of 20 nanowires of 50 nm width and 10 □m length and biased at V_{ref} = -1.5 V and V_d = 1 V is shown as a function of time. First, as a control experiment, 100 μL of plain PBS were injected separately into the main channel solution at the time mark of ~ 900 s (figure 4(b)), by the use of a T-junction. From the T-junction, the flow continued along the PE tubing (~ 1 m) into the probe station. As expected, this injection caused no significant change in the device current, see Fig. 4(b). This is a clear proof that all the subsequent signals obtained by the sensor are caused exclusively by streptavidin attachment to the nanowire surface.

After the initial plain PBS injection, 100 μL PBS solution with the lowest streptavidin concentration of 580 zM was injected into the main channel solution at the time mark of ~ 1100 s (figure 4(b)). A remarkable response of the sensor to this extremely low streptavidin concentration can be clearly seen in figure 4(b). Following this first streptavidin injection, the microfluidic channel and the device were rinsed by plain PBS for ~ 3-4 min. Then, the PBS solutions with increasing streptavidin concentrations were introduced step by step within the continuous stream of pure PBS buffer. After each streptavidin injection, the microfluidic channel and the sensor were consequently rinsed from potentially unbound streptavidin molecules by plain PBS for the same time of ~ 3-4 min. With each increasing streptavidin concentration, an increasing response of the sensor is clearly observed in figure 4(b) up to the highest concentration of 380 nM.

As mentioned above, the remarkable responses of the sensor to the streptavidin injections are reflective of the protein attached to the nanowire surface. The possible sensor response to the charged streptavidin molecules passing close to the surface of the nanowires might be ruled out for the following reason. In our experiments we used a solution of PBS with pH = 7.4 and medium range concentration of 10 mM, where the Debye screening length is $\lambda_D \approx 3.1$ nm. This means that the unbound streptavidin molecules passing by the surface of the nanowires at a distance > 3.1 nm will not have any influence on the sensor current. The ones that come closer then 3.1 nm will either bind to the biotinylated surface of the nanowires because of the extraordinarily high affinity of streptavidin for biotin or non-covalently attach to the

nanowire surface. Such a non-covalent attachment might be indicative of incomplete biotinylation of the APTES layer and may be facilitated by the expected positive charge of this layer at pH = 7.4 due to the partial protonation of its amine groups [23]. The low positive potential (in the range of few millivolts) of the APTES layer can electrostatically attract and capture the negatively charged (at pH = 7.4) streptavidin molecules. These molecules, together with the covalently bound ones, most probably cause the high peaks in the measured current observed in figure 4(b). However, the non-covalent attachment of streptavidin is weaker than the covalent binding and streptavidin molecules that are not bound to biotin can be washed off by the constantly flowing PBS. This may be the reason for the current drops after the streptavidin injections have passed over the sensor (figure 4(b)). In such a case, the "peak" current values are indicative of streptavidin molecules both covalently and non-covalently attached to the nanowire surface, whereas the "valley" current values should be indicative of streptavidin molecules covalently bound to biotin.

The dashed line (red online) in figure 4(b) extrapolates the possible current drift before the first streptavidin injection, while the solid line (light blue online) connects the "valley" current values after each streptavidin injection. When one compares the two lines, it becomes obvious that even at the level of those valleys there is a significant jump in the measured current already after the first injection with the extremely low streptavidin concentration of 580 zM, which cannot be attributed to a continuous current drift. Therefore, one could convincingly conclude that the sensor response in our case is indeed reflective of streptavidin molecules binding to the biotinylated nanowire surface.

In one of our previous works [6], we performed similar experiment using another type of sensors, namely 3D vertically stacked Si nanowire FETs. In spite of the fact that the sensing devices were quite different from the current ones and had the opposite doping (n-type instead of p-type), the results were comparable with the ones we present here and we were able to detect streptavidin at a concentration as low as 17 aM. This might be considered as an indirect proof that streptavidin can indeed be reproducibly and reliably detected at these low concentrations.

Plots of the peak current values and valley current values for each streptavidin injection as functions of the respective streptavidin concentrations are presented in figure 5. Logistic fits of the two dependences were suggested with the function

$$y = a_2 + (a_1 - a_2)/[1 + (x/x_0)^p]. \quad (1)$$

The logistic function is widely used, among others, in pharmacy and chemistry to model the concentration of reactants and products in autocatalytic reaction.

The plots in figure 5 show the distinct increase of drain current with the increase in the streptavidin concentration. There is, however, some decrease in the increment of the sensing signal current for each subsequent injection from about 25% between the first two injections to about 15% between the injections 7 and 8. This might be caused by a partial saturation of the binding sites of the self-assembled biotin monolayer. There is also a slight decrease in the peak current for the last injection of streptavidin with the highest concentration of 380 nM. It is difficult to speculate what could be the reason for this but it is definitely not a result of breaking streptavidin bonds to biotin. A possible explanation might be either oversaturation of the biotin monolayer or a partial desorption of this layer.

In figure 5 it is clearly seen that the slopes of the two curves are different: the dependence of the peak currents on streptavidin concentration is steeper than the one of valley currents. This indicates that different phenomena determine the values of the peak currents and the valley currents. As discussed above, the peak current values are most probably reflective of streptavidin molecules attached both covalently and non-covalently to the nanowire surface, whereas the values of the valley currents are reflective of streptavidin molecules covalently bound to biotin. If they were a result just of a current drift with time, they would have the same slope. This is yet another proof that the sensor response in our case is indeed reflective of streptavidin molecules binding to the biotinylated nanowire surface.

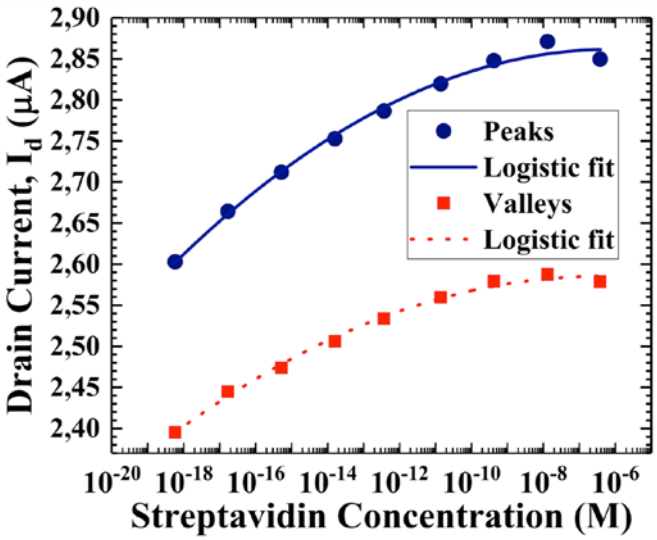

Figure 5. Plots of the dependencies of peak current values and valley current values for each streptavidin injection on the respective streptavidin concentrations.

To the best of our knowledge, the concentration of 580 zM is the lowest streptavidin concentration ever detected by any kind of sensor. At this concentration, the number of streptavidin molecules in the injected volume of the PBS solution (100 μL) was ~ 35. The upper limit estimation of the microfluidic channel volume is (W × H × L): 200 μm × 200

μm × 1 cm = 0.4 μL. This means that we had in average only one molecule (statistically less than one molecule) in the microfluidic channel at any time. In addition, the functionalisation approach used in this work implies that surface modification with APTES/biotin happens not only at the nanowires but also at the area around them, which is much larger than the NW surface itself. This fact leads to the existence of a vast number of competing sites outside the nanowires, which are capable of binding the target molecules. Statistically, the number of the binding sites outside the nanowires is greater than the number of the binding sites at the nanowires with a ratio much higher than 35:1. Moreover, due to the constant flow of the PBS solution, streptavidin has only a limited time to bind to the nanowires before the unbound molecules are carried away by the flowing PBS. Taking into account all these factors, it is possible to state with a great certainty that at the concentration of 580 zM we most probably detected only few streptavidin molecules closly approaching detection at the single molecule level.

The observed superior performance of JNT sensors might be due to at least two advantages of JNTs over the classical MOSFETs [10-13], which are especially important for their application as sensors:

(i) The current flow in JNTs is not controlled by a reverse biased p-n junction as in standard MOSFETs but entirely by the gate potential, which modulates the carrier density in the channel. Therefore, they are more sensitive to any change in the electrostatic potential on the channel surface acting as a gate potential.

(ii) JNTs demonstrate bulk conductance near the centre of the channel (NW), in contrast to the conductance in a thin surface inversion or accumulation layer near the gate in the inversion mode (IM) or accumulation mode (AM) transistors, which leads to higher drive currents. Moreover, this fact makes the modulation of depletion and the conduction in JNTs less affected by the noise-inducing parasitic surface states than in the case of conventional MOSFETs, which is very important for achieving high signal-to-noise ratio and hence the ultimate detection limit of a single molecule [7-9].

4. Conclusions

Detection of the protein streptavidin at concentration as low as 580 zM is demonstrated for the first time using junctionless nanowire transistors operated as FET-type Si NW sensors. At the particular experimental conditions of the present work, this concentration corresponds to detection of only few molecules, nearly approaching the fundamental limit of a chemo-/biosensor of detection at a single molecule level. As indicated above, the excellent sensing capabilities of JNTs are due to the fact that their performance is, on one hand, more sensitive to any change in the electrostatic potential on the channel surface and, on the other hand, is less susceptible to the noise-inducing parasitic surface states than the performance of standard MOSFETs. This is very important for achieving high signal-to-noise ratio towards the ultimate detection limit of a single molecule. Thus the performance advantages of JNT sensors over the standard FET-type Si NW sensors, together with their very simple structure and relaxed fabrication process make them excellent candidates for low-cost mass production by the conventional semiconductor technology. Therefore, the results presented here can open the way to numerous applications of JNT sensors in various fields where fast, low-cost, label-free, low-volume and real-time detection of chemical and biological species at the fundamental limit of a single molecule is required.

Acknowledgements

The authors would like to acknowledge funding from the EU 7th Framework Programme under the SiNAPS project (no. 257856) and the Science Foundation Ireland (SFI) under the grant no. 09/IN.1/I2602.

References

[1] Cui Y, Wei Q, Park H and Lieber C M 2001 Nanowire nanosensors for highly sensitive and selective detection of biological and chemical species *Science* **293** 1289–1292

[2] Chen K I, Li B R and Chen Y T 2011 Silicon nanowire field-effect transistor-based biosensors for biomedical diagnosis and cellular recording investigation *Nano Today* **6** 131–154

[3] Cao A, Sudhölte E J R and de Smet L C P M 2014 Silicon Nanowire-Based Devices for Gas-Phase Sensing *Sensors* **14** 245-271

[4] Patolsky F, Zheng F, Hayden O, Lakadamyali M, Zhuang X and Lieber C M 2004 Electrical detection of single viruses *ProcNatlAcadSciUSA* **101** 14017–14022

[5] Stern E, Klemic J F, Routenberg D A, Wyrembak P N, Turner-Evans D B, Hamilton A D, LaVan D A, Fahmy T M and Reed M A 2007 Label-free Immunodetection with CMOS-Compatible Semiconducting Nanowires *Nature* **445** 519-522

[6] Buitrago E, Fernandez-Bolaños M, Georgiev Y M, Yu R, Lotty O, Holmes J D, Nightingale A M and Ionescu A M 2014 Attomolar Streptavidin and pH, Low Power Sensor Based on 3D Vertically Stacked SiNW FETs, *Conf. Proc. of the Internat. Symp. on VLSI Technol., Syst. and Appl. (VLSI-TSA)*, Hsinchu, Taiwan, 28-30 April 2014, 147-148

[7] Rajan N K, Routenberg D and Reed M 2011 Optimal signal-to-noise ratio for silicon nanowire biochemical sensors *Appl. Phys. Lett.* **98** 264107−2641073

[8] Bedner K *et al* 2014 Investigation of the dominant 1/f noise source in silicon nanowire sensors *Sensor, Actuat. B-Chem.* **191** 270-275

[9] Pud S. *et al* 2014 Liquid and Back Gate Coupling Effect: Toward Biosensing with Lowest Detection Limit *Nano Lett.* **14** 578-584
[10] Colinge J P *et al* 2010 Nanowire transistors without junctions *Nature Nanotech.* **5** 225-229
[11] Colinge J P, Lee C W, Akhavan N D, Yan R, Ferain I, Razavi P, Kranti A and Yu R 2011 Junctionless Transistors: Physics and Properties *Semiconductor-On-Insulator Materials for Nanoelectronics Applications* Nazarov A. *et al.* eds. Springer-Verlag Berlin Heidelberg pp 187-200
[12] Colinge J P, Kranti A, Yan R, Lee C W, Ferain I, Yu R, Akhavan N D and Razavi P 2011 Junctionless Nanowire Transistor (JNT): Properties and design guidelines *Solid State Electron.* **65–66** 33
[13] Georgiev Y M, Yu R, Petkov N, Lotty O, Nightingale A M, deMello J C, Duffy R and Holmes J D 2014 Silicon and Germanium Junctionless Nanowire Transistors for Sensing and Digital Electronics Applications *Functional Nanomaterials and Devices for Electronics, Sensors and Energy Harvesting* Nazarov A. *et al.* eds. Springer International Publishing AG, Cham, Switzerland ch 17 pp. 367-388.
[14] Gao X P A, Zheng G and Lieber C M Subthreshold Regime has the Optimal Sensitivity for Nanowire FET Biosensors *Nano Lett.* **10** 547-552
[15] Buitrago E, Fagas G, Fernández-Bolanos Badia M, Georgiev Y M, Berthomé M and Ionescu A M 2013 Junctionless silicon nanowire transistors for the tunable operation of a highly sensitive, low power sensor *Sensor. Actuat. B-Chem.* **183** 1– 10
[16] Yu R, Georgiev Y M, Lotty O, McCarthy B, Petkov N, O'Connell D, Nightingale A M, Das S and Holmes J D 2013 Silicon Junctionless Transistor for Sensing Application: Subthreshold Region Sensor *Proceedings of the Ninth Workshop of the Thematic Network on Silicon on Insulator Technology, Devices and Circuits (EUROSOI)*, Paris, France, Jan 21-23, 2013
[17] Georgiev YM, Petkov N, McCarthy B, Yu R, Djara V, O'Connell D, Lotty O, Nightingale A M, Thamsumet N, deMello J C, Blake A, Das S and Holmes J D 2014 Fully CMOS-compatible top-down fabrication of sub-50 nm silicon nanowire sensing devices *Microelectron. Eng.* **118** 47-53
[18] Georgiev Y M, Henschel W, Fuchs A and Kurz H 2005 Surface Roughness of Hydrogen Silsesquioxane as a Negative Tone Electron Beam Resist *Vacuum* **77** 117-123
[19] Henschel W, Georgiev Y M and Kurz H 2003 Study of a High Contrast Process for Hydrogen Silsesquioxane as a Negative Tone Electron Beam Resist *J Vac Sci Technol B* **21** 2018-2025
[20] Ong H G *et al* 2011Origin of Hysteresis in the Transfer Characteristic of Carbon Nanotube Field Effect Transistor *Journal of Physics D: Applied Physics* **44** 285301
[21] Park I Y, Li Z Y, Pisano A P and Williams R S 2010 Top-down Fabricated Silicon Nanowire Sensors for Real-time Chemical Detection *Nanotechnology* **21** 015501
[22] Duan X, Yue L, Rajan N K, Routenberg D A, Modis Y and Reed M A 2012 Quantification of the Affinities and Kinetics of Protein Interactions Using Silicon Nanowire Biosensors *Nat. Nano.* **7** 401-407
[23] Gijs, M A M, Applications of Magnetic Labs-on-Chips, in Kakaç S, Kosoy B, Li D, Pramuanjaroenkij A, eds. Microfluidics Based Microsystems: Fundamentals and Applications. Springer Science & Business Media, 2010, p. 459